THE INFLUENCE OF DUST ON MARTIAN OZONE DETECTION.

D. G. Dawson, M. R. Patel, S. R. Lewis, J. P. Mason, *Department of Physical Sciences, The Open University, Walton Hall, Milton Keynes MK7 6AA, UK*, **P. G. J. Irwin,** *Atmospheric, Oceanic and Planetary Physics, Clarendon Laboratory, University of Oxford, Parks Road, Oxford OX1 3PU, UK*, **A. C. Vandaele,** *IASB-BIRA, Brussels, Belgium*.

Introduction

The principal contributors to variations in the ultraviolet environment of Mars are ozone and dust. Ozone is a strong absorber of ultraviolet (UV) light, resulting in a reduction in transmitted radiance in the wavelength region surrounding 255 nm. The spatio-temporal distribution of ozone may be investigated by comparing spectral observations from Mars orbit with solar reference spectra. The photoionisation of molecular species in the upper atmosphere is driven by high energy solar UV radiation, therefore the photochemical role of ozone is a prominent component of the complex system of chemical reactions regulating the atmospheric system.

The effect of dust on observed radiance from orbit is a factor in the accuracy of ozone abundance retrievals, particularly at high solar zenith angles (decreased radiance and increased scattering) or high dust loading conditions. The aim of this work is to apply varying dust aerosol distributions, concentrations, and properties to a library of ozone vertical profiles (with consistent atmospheric structures) in order to quantify the effect of dust on future ozone abundance retrievals.

NOMAD-UVIS

The European Space Agency and Roscosmos ExoMars Trace Gas Orbiter (TGO) mission is due to launch in 2016. Its scientific goals include the investigation of trace gases in the atmosphere, in part looking for past or present signatures of active biological or geological processes. Mapping the spatio-temporal distribution of trace gases and their source regions will be undertaken, providing insight into data assimilation models to investigate atmospheric circulation. In addition, the spacecraft will deploy the Entry, descent, and landing Demonstrator Module (EDM), and act as a data relay for the 2018 ExoMars Rover.

The TGO payload includes the NOMAD 3-channel spectrometer suite (**N**adir and **O**ccultation for **MA**rs **D**iscovery). The UVIS channel of NOMAD has a 200 - 650 nm range with 1.5 nm resolution for nadir and solar occultation observations. The scientific goals of UVIS are to improve the understanding of martian photochemistry, to characterize and map aerosols, and to investigate other minor species. This work supports the development and future operation of the UVIS instrument through simulating observations using a radiative transfer model.

Radiative transfer model

NEMESIS (**N**on-linear optimal **E**stimator for **M**ultivariat**E** **S**pectral analy**SIS**) (Irwin et al., 2008) is a general purpose retrieval model applicable to any planetary atmosphere, having been initially developed alongside the Composite InfraRed Spectrometer (CIRS) on the NASA Cassini mission to the Saturn system. NEMESIS is both a forward model, generating a synthetic spectrum from a provided atmospheric structure, and a retrieval model, adjusting atmospheric parameters until differences between observed and synthetic spectra are minimised. The model has been extended for the martian UV environment through the inclusion of appropriate gaseous absorption data and airborne dust optical properties as part of this work.

Output from the Mars Climate Database (Lewis et al., 1999, version 5) is used to provide atmospheric vertical structures. The assumed nominal martian year is an ensemble average of LMD GCM (Global Circulation Model) simulations using dust distributions observed during (the non dust storm) Mars Years 24, 26, 27, 29, and 30, with solar average conditions.

The modelled spectral range includes the UVIS wavelengths and extends into the near infrared (200 - 1100 nm) for a wider context on the spectral influence of suspended dust. In the visible and NIR region, HiTran data are used to produce k-tables for H_2O, CO_2, and O_2 using the method of correlated-k (Irwin et al., 2008; Lacis & Oinas, 1991). The resulting temperature and pressure dependent look-up tables increase computational speed, at a cost of knowing the precise wavelength location of absorption coefficients. In the UV where HiTran data are not available, absorption cross-sections are used in the continuum part of the calculation for O_3, CO_2, O_2, and SO_2. The volume mixing ratios of each gas vary as a function of height, as defined by the MCD profile used for a particular run.

The surface albedo as a function of wavelength is interpolated from Mallama (2007) at wavelengths of 360, 440, 550, 700, and 900 nm from numerous ground observations from the 1950s up to 2006. The range used in this study has been extended (Otter, 2009) using the ground observations of Esposito et al. (2007) and Fox et al. (1997).

Ozone

The detection of ozone on Mars was first achieved by the Mariner 7 and 9 flyby missions (Barth & Hord, 1971; Barth et al., 1973), and subsequently from martian orbit by Mars 5 (Krasnopolsky & Parshev, 1979), Phobos 2 (Blamont & Chassefière, 1993), and Mars Express (Bertaux et al., 2006). Measurements have also been made from the Earth's surface (Espenak et al., 1991; Novak et al., 2002; Fast et al., 2006), and Earth orbit (Clancy et al., 1999). NASA's Curiosity Rover contains the first *in situ* UV (photodiode) detector, however a dedicated UV spectrometer has yet to be placed on the surface, and orbital observations with global coverage remain the best method of assessing the UV environment of Mars.

Due to the anti-correlation of ozone with water vapour, ozone is most abundant near the poles in winter, when the water vapour has condensed to the polar ice caps, leading to significant increases in ozone abundance at $L_s = 225$ to $315°$ (northern winter) and $L_s = 45$ to $135°$ (southern winter). Figure 1 shows the modelled latitudinal distribution of ozone over a typical martian year from MCD output.

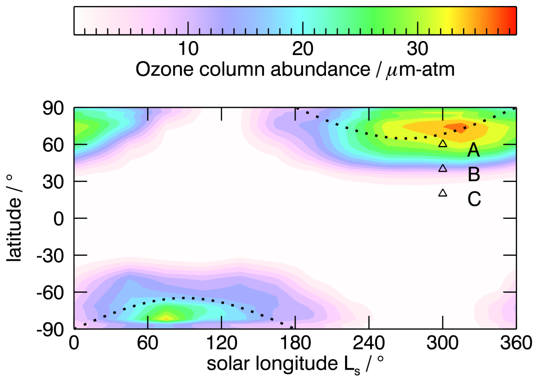

Figure 1: Ozone column abundance over a nominal martian year from MCD output, longitudinally averaged at local noon. The dotted lines enclose the polar night. Sites A, B, and C (latitudes = 60°, 40° 20°, L_s = 300°) are marked for discussion.

The vertical profile of ozone is non-uniform, and is most abundant near the surface, typically below 20 km. Often a second peak is formed at approximately 50 km. For the nadir observations considered in this study, the precise vertical profile is secondary to recovering accurate total column abundances. In order to determine the effect of dust loading on the accuracy of ozone abundance retrieval, a library of appropriate MCD atmospheric vertical profiles has been produced as part of this work. These scenarios are representative of the seasonal, diurnal, and latitudinal variations in martian atmospheric structure.

Dust

The amount of airborne dust varies over the martian year, with the column optical depth reaching a maximum during the southern summer. However, this is for a nominal year; an interannual variation in dust content exists particularly in the southern summer. Dust storms potentially lasting many months and engulfing the planet can dramatically increase the optical depth. To account for these large variations, large optical depths ($0 < \tau < 5$) are considered for this study. The dust size distribution dependence on altitude has not been considered here, but will be applied to future studies on the spectral influence of discrete dust layers.

The dust model uses the complex indices of refraction derived by Wolff et al. (2009, 2010). Mie scattering for spherical particles is implemented as an approximation to an ensemble of irregularly shaped particles. The particle size distribution is assumed to have effective radius $r_{\text{eff}} = 1.6$ μm and effective variance $\nu_{\text{eff}} = 0.3$ (Wolff et al., 2009, 2010), and to follow a standard gamma distribution. Cloud aerosols are not included at this time, and will be implemented in future work.

Modelling

Preliminary modelling to simulate an observed spectrum is shown in Figure 2 (at site B of Figure 1). This is the simulated radiance measured by an instrument in Mars orbit, transmitted through an MCD derived atmospheric state, determining the effect of this atmosphere on the reflected solar spectrum observed in nadir geometry. The dust content of the atmosphere is increased by scaling the dust vertical concentration profile to obtain the reported column optical depths. The increasing radiance with increasing dust content is apparent, particularly at longer red wavelengths where the albedo of both the surface and lofted dust is greater. The characteristic 255 nm ozone absorption feature becomes more difficult to discern with increasing dust, especially during extreme events. Simulated observations at sites A and C return similar results with variation in the size of the ozone absorption feature.

The size of the ozone peak, indicative of ozone abundance, can be measured by taking the ratio of radiances at wavelengths of 255 and 290 nm. This compares the radiance at the peak to the radiance at a wavelength both sufficiently far from significant ozone absorption, and sufficiently close to minimize wavelength variation in dust optical properties. Figure 3 shows this radiance ratio, normalized by the solar spectrum, as a function of dust opacity τ. For sites A and B the ozone feature is reduced in magnitude to 60% when the dust content is increased from τ = 0.1 to 1.0. This is significant as measurements by the Spirit and Opportunity rovers

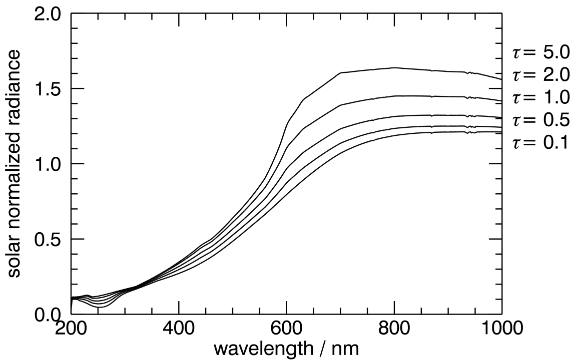

Figure 2: The simulated radiance has been normalized by the solar spectrum, and such that the low dust case has a radiance of unity at 670 μm. The spectrum at site B of Figure 1 is shown, where L_s = 300°, latitude = 40°, and solar zenith angle = 61.6° (local noon). Increasing the dust content τ and therefore the number of scattering events increases the radiance, particularly towards red wavelengths. The dust column optical depths increase from τ = 0.1 (low dust), to τ = 5 (dust storm).

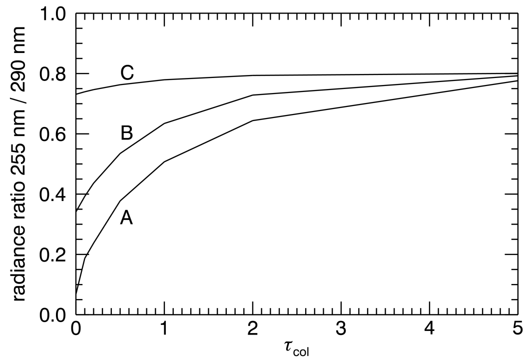

Figure 3: The radiance ratio is of the solar normalized radiance at wavelengths of 255 and 290 nm; shown here as a function of dust opacity τ at sites A, B, and C of Figure 1. The ratio is a measure of the absorption due to ozone, with greater absorption giving a smaller ratio. As τ increases the feature becomes less defined as it is obscured by dust aerosol scattering.

have shown that dust column optical depths consistently approach 1.0 for over a third of the martian year (Lemmon, 2004), and therefore ozone abundances are likely to be underestimated. For site C the ozone feature is reduced in magnitude to 85%, this a consequence of the smaller ozone abundance, and does not mean accuracy is greatest at site C.

The degradation of the ozone absorption feature is a result of increased scattering of light by aerosols, this scattered light replaces the light lost due to ozone absorption. The asymptotic trend towards a ratio of 0.8 is a result of the optical properties of dust at those wavelengths and the complete obfuscation of ozone. Incorporating clouds and considering the global and seasonal variation in ozone and dust profiles will result in characterizing to what extent ozone observations will be impeded throughout the martian year.

Conclusion

The continued monitoring of ozone of Mars is essential to the understanding of its photochemical role, and to defining the level of spectral protection afforded to any potential biological activity in the martian regolith. Quantifying the effect of dust on retrieving accurate ozone abundances is a critical part of this process, particularly at high latitudes with larger ozone abundances and higher solar zenith angles. Characterizing the effect of varying aerosol optical properties, size distributions, and the surface treatment on spectra such as in Figure 2 will increase our understanding, and therefore the quality, of ozone retrievals from multiple observations. The relationship between the signal to noise ratio of NOMAD-UVIS and the detection limits of ozone and other trace gases will also be determined.

References

Barth, C. A. & Hord, C. W. (1971), 'Mariner Ultraviolet Spectrometer: Topography and Polar Cap', *Science* **173**, 197–201.

Barth, C. A., Hord, C. W., Stewart, A. I. & Lane, A. L. (1973), 'Mariner 9 Ultraviolet Spectrometer Experiment: Observations of Ozone on Mars', *Icarus* **18**, 102–108.

Bertaux, J. L., Korablev, O., Perrier, S., Quèmerais, E., Montmessin, F., Leblanc, F., Lebonnois, S., Rannou, P., Lefèvre, F., Forget, F., Fedorova, A., Dimarellis, E., Reberac, A., Fonteyn, D., Chaufray, J. & Guibert, S. (2006), 'SPICAM on Mars Express: Observing modes and overview of UV spectrometer data and scientific results', *J. Geophys. Res.* **111**, E10S90.

Blamont, J. E. & Chassefière, E. (1993), 'First detection of ozone in the middle atmosphere of Mars from solar occultation measurements', *Icarus* **169**, 311–323.

Clancy, R. T., Wolff, M. J. & James, P. B. (1999), 'Minimal Aerosol Loading and Global Increases in Atmospheric Ozone during the 1996-1997 Martian Northern Spring Season', *Icarus* **138**, 49–63.

Espenak, F., Mumma, M. J., Kostiuk, T. & Zipoy, D. (1991), 'Ground-Based Infrared Measurements of the Global Distribution of Ozone in the Atmosphere of Mars', *Icarus* **92**, 252–262.

Esposito, F., Giuranna, M., Maturilli, A., Palomba, E., Colangeli, L. & Formisano, V. (2007), 'Albedo and photometric study of Mars with the Planetary Fourier Spectrometer on-board the Mars Express mission', *Icarus* **186**(2), 527 – 546.

Fast, K., Kostiuk, T., Espenak, F., Annen, J., Buhl, D., Hewagama, T., A'Hearn, M. F., Zipoy, D., Livengood, T. A., Sonnabend, G. & SchmÃ…lling, F. (2006), 'Ozone abundance on Mars from infrared heterodyne spectra I: Acquisition, retrieval, and anticorrelation with water vapor', *Icarus* **181**, 419–431.

Fox, G. K., Code, A. D., Anderson, C. M., Babler, B. L., Bjorkman, K. S., Johnson, J. J., Meade, M. R., Nordsieck, K. H., Sanders, W. T., Weitenbeck, A. J., Zellner, N. E. B., Edgar, R. J. & Lupie, O. L. (1997), 'Solar System Observations by the Wisconsin Ultraviolet Photopolarimeter Experiment.I.The First Ultraviolet Linear Spectropolarimetry of Mars', *The Astronomical Journal* **113**, 1152–1157.

Irwin, P. G. J., Teanby, N. A., deKok, R., Fletcher, L. N., Howett, C. J. A., Tsang, C. C. C., Wilson, C. F., Calcutt, S. B., Nixon, C. A. & Parrish, P. D. (2008), 'The NEMESIS planetary atmosphere radiative transfer and retrieval tool', *Journal of Quantitative Spectroscopy & Radiative Transfer* **109**, 1136–1150.

Krasnopolsky, V. A. & Parshev, V. A. (1979), 'Ozone and photochemistry of the martian lower atmosphere', *Planetary and Space Science* **27**, 113–120.

Lacis, A. A. & Oinas, V. (1991), 'A Description of the Correlated k Distribution Method for Modeling Nongray Gaseous Absorption, Thermal Emission, and Multiple Scattering in Vertically Inhomogeneous Atmospheres', *J. Geophys. Res.* **96**, 9027–9063.

Lemmon, M. T. (2004), 'MER Mars Pancam Atmospheric Opacity RDR V1.0, NASA Planetary Data System, MER1/MER2-M-PANCAM-5-ATMOS-OPACITY-V1.0'.

Lewis, S. R., Collins, M., Read, P. L., Forget, F., Hourdin, F., Fournier, R., Hourdin, C., Talagrand, O. & Huot, J.-P. (1999), 'A climate database for Mars', *J. Geophys. Res.* **104**, 24177–24194.

Mallama, A. (2007), 'The magnitude and albedo of Mars', *Icarus* **192**, 404–416.

Novak, R. E., Mumma, M. J., DiSanti, M. A., Dello Russo, N. & Magee-Sauer, K. (2002), 'Mapping of Ozone and Water in the Atmosphere of Mars near the 1997 Aphelion', *Icarus* **158**, 14–23.

Otter, S. (2009), 'Simulation of the Radiative Flux at the Martian Surface between 180 and 1100 nm', *PhD Thesis, Open University*.

Wolff, M. J., Clancy, R. T., Goguen, J. D., Malin, M. C. & Cantor, B. A. (2010), 'Ultraviolet dust aerosol properties as observed by MARCI', *Icarus* **208**, 143–155.

Wolff, M. J., Smith, M. D., Clancy, R. T., Arvidson, R., Kahre, M., Seelos, F., Murchie, S. & Savijarvi, H. (2009), 'Wavelength dependence of dust aerosol single scattering albedo as observed by the Compact Reconnaissance Imaging Spectrometer', *J. Geophys. Res.* **114**, E00D04.